Event-Based Validation of Swell Arrival Time

HAOYU JIANG

*Department of Marine Technology, College of Information Science and Engineering, Ocean University of China,
Qingdao, China, and Centre for Ocean Engineering, Science and Technology,
Swinburne University of Technology, Melbourne, Victoria, Australia*

ALEXANDER V. BABANIN

*Department of Infrastructure Engineering, Melbourne School of Engineering, University of Melbourne, and
Centre for Ocean Engineering, Science and Technology, Swinburne University of Technology,
Melbourne, Victoria, Australia*

GE CHEN

*Department of Marine Technology, College of Information Science and Engineering, Ocean University of China, and
Laboratory for Regional Oceanography and Numerical Modeling, Qingdao National Laboratory for
Marine Science and Technology, Qingdao, China*

ABSTRACT

The arrival time of ocean swells is an important factor for offshore and coastal engineering and naval and recreational activities, which can also be used in evaluating the numerical wave model. Using the continuity and pattern of wave heights during the same swell event, a methodology is developed for identifying swell events and verifying swell arrival time in models from buoy data. The swell arrival time in a WAVEWATCH III hindcast database is validated with in situ measurements. The results indicate that the model has a good agreement with the observations but usually predicts an early arrival of swell, about 4 h on average. A histogram shows that about one-quarter of swell events arrive early and three-quarters late by comparison with the model. Many processes that may be responsible for the arrival time errors are discussed, but at this stage it is not possible to distinguish between them from the available data.

1. Introduction

Storms in the ocean can generate long surface gravity waves propagating away from their sources as swells. These waves can propagate over thousands of kilometers with little energy loss (e.g., Snodgrass et al. 1966; Collard et al. 2009; Ardhuin et al. 2009), radiating momentum and energy across ocean basins (Munk et al. 1963). Swells have impacts on many aspects of the human life from industrial activities such as port operations to recreational activities such as surfing. They are also important to many physical processes of the Earth system such as momentum exchange at the air–sea boundary and sediment transport in the coastal areas.

The studies of swells and their forecast have been conducted since the 1940s (e.g., Barber and Ursell 1948; Rogers et al. 2014). Through years of development, numerical wave models nowadays can give a fairly good forecast of many swell parameters compared with observations (e.g., Ardhuin et al. 2010; Zieger et al. 2015). To evaluate or verify a numerical model, the observed wave parameters are usually collocated with the model outputs in the same time and location, and comparisons are made between two sets of data. However, as the swells can travel large distances, the arrival time of a swell event should also be taken into consideration when evaluating a model. The arrival time of swells itself is a very practical parameter as many human activities are time sensitive, such as arranging enough time for contingency plan or forecasting the best time for surfing.

Some previous studies mentioned the idea of swell arrival time (Wingeart et al. 2001; Delpey et al. 2010;

Ardhuin et al. 2016) and anecdotal pieces of evidence are full of stories of both early and late arrival of swells by comparison with the model forecast. However, it seems there is still no clear definition of the "arrival time" of swell, which makes it hard to do the comparison quantitatively. The aim of this study is trying to present a consistent and robust method to validate the model performance for the arrival time of swells. Using this method, we also identified the problem of the swell early/late arrival that needs to be explained and solved in the future.

2. Data and methods

a. Data

To investigate the arrival time of swells, the variation of wave information against time, that is, a successive time series, is needed. Quality controlled in situ measurements from the National Data Buoy Center (NDBC) are employed as the reference data for the model output. To compare with the global model output, 13 deep-water buoys (Table 1) sufficiently far from the coastlines with directional spectral information available are selected. The directional spectra are reconstructed using Earle et al. (1999) and are smoothed using a 3-h running average and then partitioned using the procedure of Portilla et al. (2009).

The model hindcast data here are two-dimensional spectra computed by WAVEWATCH III (WW3) with the physical parameterization of Ardhuin et al. (2010). The outputs are selected in the buoys' locations from 2000 to 2012 with a time resolution of 1 h, and the spectra are also partitioned by the procedure of Portilla et al. (2009). The data are downloaded from the L'Institut Français de Recherche pour l'Exploitation de la Mer (Ifremer) ftp server where more detailed information is available (Rascle and Ardhuin 2013).

b. Swell event identification and collocation

Wave information at a given location from the same meteorological event (e.g., an extratropical storm) is organized into one time series that is regarded as a wave event. This event assignment is operated using the wave tracking technology proposed by Hanson and Phillips (2001, in their section 2b). After the wave tracking procedure, three criteria are adopted to filter the noises and wind-sea events, as we only focus on the arrival time of swells: 1) The maximum of the peak periods needs to be more than 12 s. 2) The duration of the event should be more than 60 h. 3) The peak frequencies in the same event need to rise significantly (p value is 0.01) with time. After that, the event from the buoy is collocated with the event from the model if 1) the two events have more than 45-h intersections in the range of time and

TABLE 1. Details of NDBC directional buoys.

Buoy ID	Location	Water depth (m)	Data period
32012	19.63°S, 84.95°W	4551	2007–09
46011	34.96°N, 121.02°W	465	2006–12
46012	37.36°N, 122.88°W	209	2011/12
46015	42.76°N, 124.83°W	420	2008–11
46050	44.68°N, 124.52°W	137	2008–10
46086	32.49°N, 118.04°W	1829	2004–12
46089	45.89°N, 125.82°W	2293	2005
51000	23.54°N, 153.81°W	4845	2009–12
51001	24.39°N, 162.13°W	4869	2006–09
51004	17.60°N, 152.40°W	5230	2011/12
51028	0.00°, 153.91°W	4747	2000–08
51100	23.56°N, 153.90°W	4755	2009–12
51101	24.32°N, 162.23°W	4837	2009–12

2) the difference in average swell wave height, peak frequencies, and peak wave directions between the two events within the time intersections are less than 1 m, 0.02 Hz, and 30°, respectively.

Three examples of collocated swell events are illustrated in Fig. 1 showing the effectiveness of the method. Some fundamental features of swell events are nicely shown in both datasets: the peak frequency increases nearly linearly with time due to the deep-water dispersion relation, while the peak directions vary in a small range, especially those from the model. The variation of wave height generally behaves as a convex function of time that first increases since the forerunner's arrival and then decays after the energy peak of the wave group passed.

c. Arrival time difference

There seems to be no recognized definition of swell arrival time. Wingeart et al. (2001) simply use the time when a swell event is detected. This method depends much on the sensitivity of the measurement, as the forerunner of a swell event usually has low energy. For instance, in Fig. 1f, the first detected wave height in the model is 0.5 m, while that of the buoy is 0.3 m. Delpey et al. (2010) defined different arrival time for different wave periods. However, people care more about the arrival of swell energy in most applications, and as the peak frequency rises nearly linearly with time, it might be hard to distinguish between the early/late arrival of swells and the overestimation/underestimation of peak frequency. Ardhuin et al. (2016) used the time of swell energy peak as the arrival time, as the energy evolution is in general a convex function against time and the peak energy is large enough to be detected. Yet, sometimes there is more than one energy peak in the data (e.g., Fig. 1e), and the peak might be not very sharp (e.g., Fig. 1f).

A swell event from a storm usually lasts several days with wave parameters varying continuously with time.
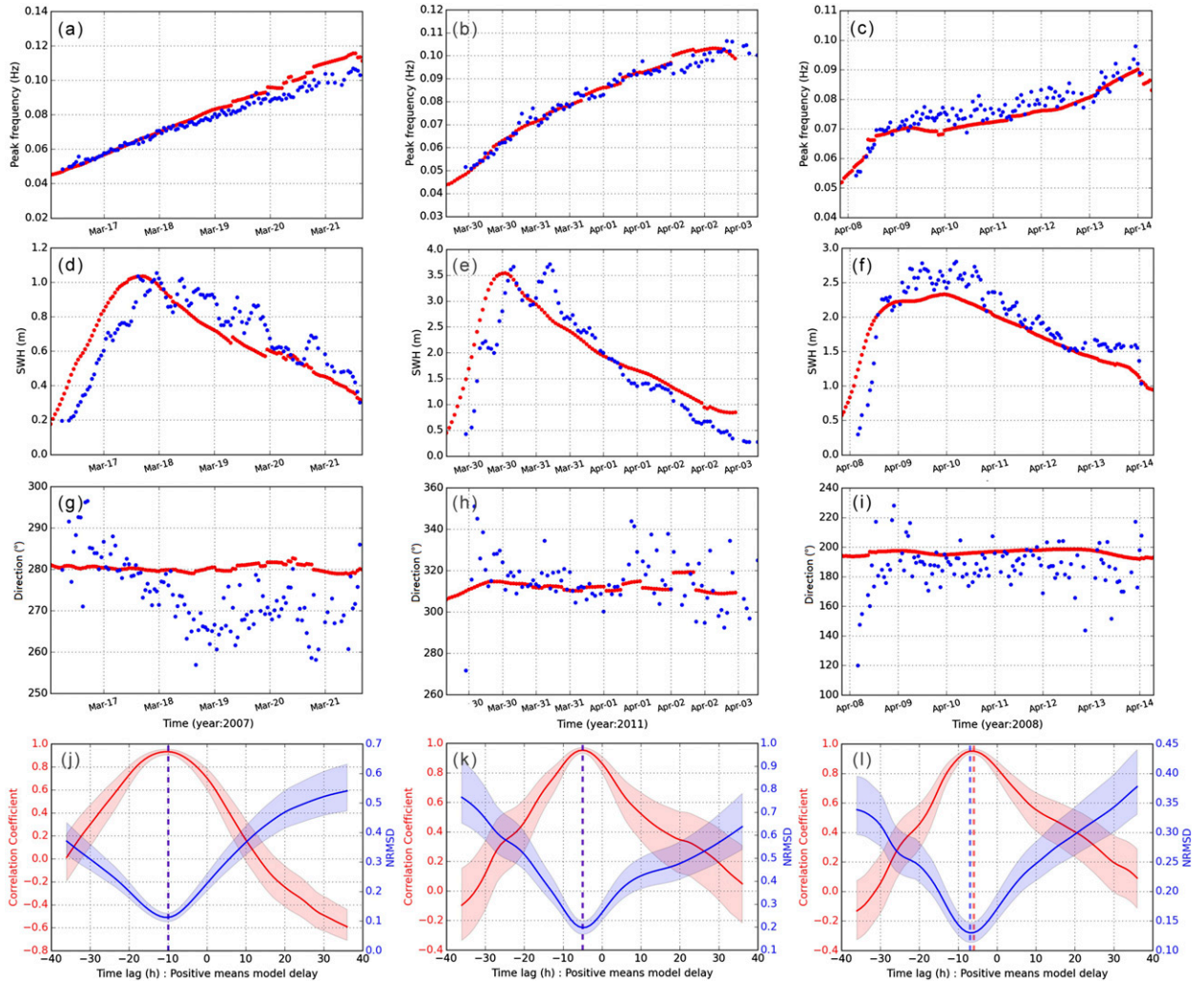
FIG. 1. (a)–(c) Peak frequencies , (d)–(f) wave heights, (g)–(i) peak directions, and (j)–(l) arrival time differences of collocated swell events from NDBC platform (left) 46086 in 2007, (center) 51101 in 2011, and (right) 32012 in 2008; in the first three rows, the blue dots are buoy measurements and the red dots are model outputs. In the fourth row, the red lines are the moving correlation coefficients and the blue lines are the moving NRMSDs [see Eqs. (1) and (2) for the definitions], and the shadow areas represent the 95% confidence intervals. The respective dot vertical lines are where the maximum of moving correlation coefficients and the minimum of moving NRMSDs appear.

It is not practical or necessary to define the point in time of the swell arrival. To validate the model, it is more important to know the difference of swell arrival time between model and observation. Here, we use wave heights to estimate this time difference, because 1) it is the best-forecasted wave parameters until now (e.g., Stopa et al. 2015), and 2) its variation is in general a convex function with more features to match between the model and the observation and is not sensitive to the systematical errors. We use two schemes to define the arrival time difference by 1) the maximum of normalized cross correlation and 2) the minimum of shift of the normalized root-mean-square difference (NRMSD):

$$r(\tau) = \frac{\sum\limits_{t=1}^{n} [H_B(t-\tau) - \overline{H_B}][H_M(t) - \overline{H_M}]}{\sqrt{\sum\limits_{t=1}^{n} [H_B(t-\tau) - \overline{H_B}]^2} \sqrt{\sum\limits_{t=1}^{n} [H_M(t) - \overline{H_M}]^2}}, \quad \text{and}$$

$$\tag{1}$$

$$\sigma(\tau) = \sqrt{\frac{\sum\limits_{t=1}^{n} [H_B(t-\tau) - H_M(t)]^2}{n\overline{H_B}^2}}, \tag{2}$$

where $H_B(t)$ and $H_M(t)$ are the time series of swell heights from the buoy and the model, respectively, for a given swell event, τ is the shifting time of buoy
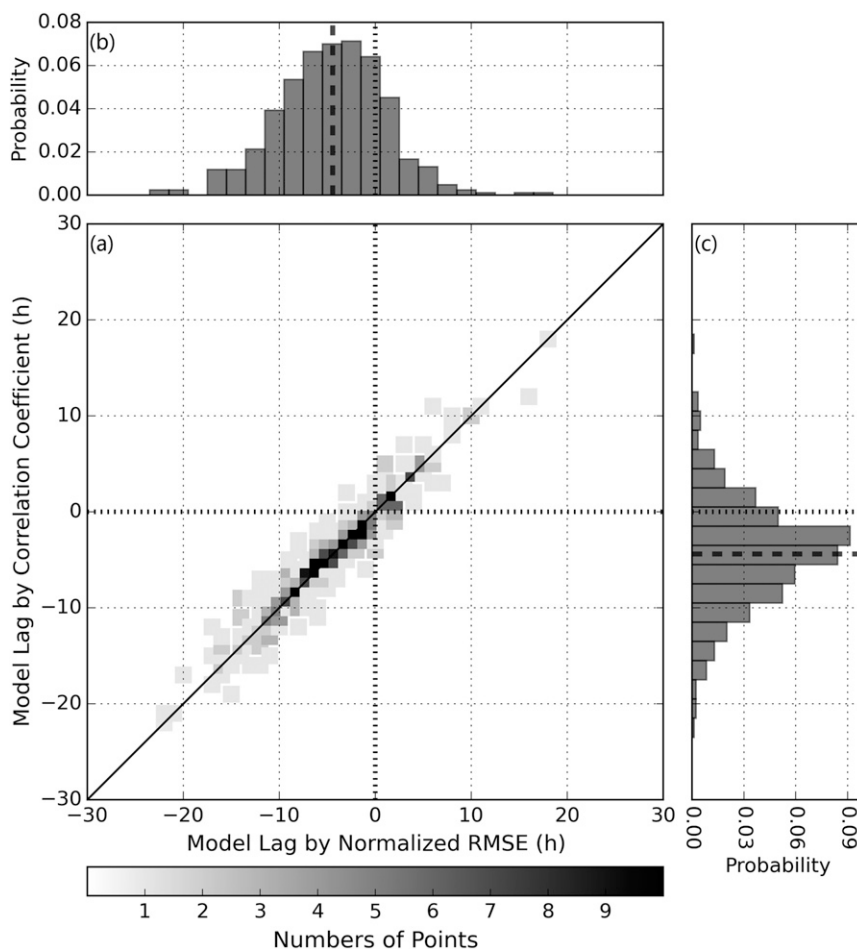
FIG. 2. (a) The scatterplot of the arrival time differences defined by shifting NRMSD vs those
defined by cross correlation; (b),(c) respective histograms of arrival time differences.

measurements, and *n* is the time span when model outputs and buoy measurements overlap. The variation of cross correlation and NRMSD are almost symmetrical with respect to each other; thus, these two definitions are consistent (the fourth line of Fig. 1). Using this consistency, some wrong-identified and wrong-collocated events are excluded from our dataset; if the time difference defined by the NRMSD corresponds to a correlation coefficient significantly smaller than the maximum (*p* value is 0.05), the collocated data pair will be eliminated from our analysis and vice versa.

3. Results and discussion

Using the above method, 421 collocated swell events are captured to estimate the arrival time difference between the model and observation. The distribution of the difference in swell arrival time of all these cases is

shown in Fig. 2. The scatterplot (Fig. 2a) demonstrates that the results derived from the two definitions are consistent. In 331 cases out of 421, the estimated time lags are within 1 h, showing the validity of the definition of the arrival time difference. Regarding the distributions of the arrival time errors in the model, both the histograms of Figs. 2b and 2c show a unimodal distribution that can be regarded as normal with a mean value of about minus 4 h, and about three-quarters of the data show the minus time differences in the model (i.e., swell arrives early in the model compared with the observations). As there is no other systematic and quantitative validation of numerical wave models from the perspective of time, there is no specific reference for the model's performance regarding swell arrival time. Considering the swells have usually propagated for more than 100 h before reaching the buoys, this is a small error. But for practical purposes, the difference of several hours can be significant. The result indicates that the swell arrival on
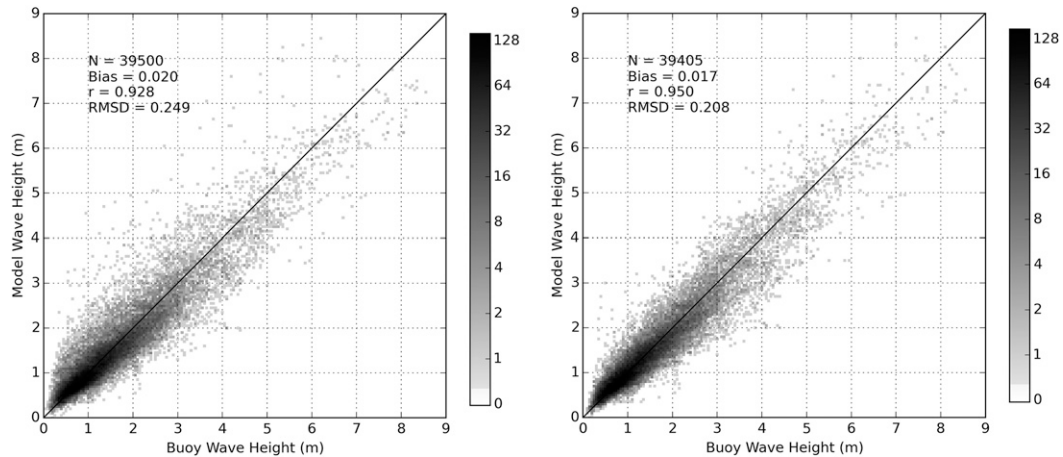
FIG. 3. The scatterplot of collocated wave heights of WW3 hindcast against NDBC buoys for the 421 swell events (a) without any correction and (b) after shifting the wave heights sequence with the arrival time difference.

average tends to delay with respect to the model forecast, at least at the given observational locations.

The wave height comparison of these 421 swell events between model output and buoy observation is shown in Fig. 3a, from which it is clear that the model can give quite good results for wave height. But after shifting the wave heights' sequence with the arrival time difference (here, we use the average of the two time differences), the result can be even further improved. After the correction in Fig. 3b, the total number of collocated pairs N is reduced by 95, but the correlation coefficient r between the two series increases, the RMSD between them decreases significantly, and the bias between the two datasets also decreases. The suspected outliers in Fig. 3a especially are all eliminated in Fig. 3b. These features all demonstrate that the differences in the arrival time of swell between model and observation are authentic, not due to the noises or errors in the observation.

Considering that the swell can propagate over thousands of kilometers, a small difference in wave parameters related to propagation such as wave direction and the group speed can be magnified over such long distances. Although the propagation of the wave is understood from first principles, there are many potential possibilities to explain the differences in swell arrival time. One category of the possibilities is that the error is embedded in the generation area of the swells. A possible reason is that there might be time lags on the arrival time of storms generating the swells. The errors of wind input, resonant wave–wave interaction, and dissipation source terms can also lead to errors in energy distributions along different frequencies, which will all impact the swell arrival time. Another category of possibilities is that the error is due to the processes in propagation, such as nonbreaking dissipation, wave–current

interactions, or some nonlinear effects. According to Ardhuin et al. (2009) or Babanin (2012), the swells with higher frequencies have higher dissipation rates, which may cause the downshifting of the energy peak along frequency in the swell field and "accelerate" the swells. Large-scale currents can impact the absolute group speed through the Doppler effect, while mesoscale eddies could refract the swells (Gallet and Young 2014), shortening or prolonging the propagation time of swells. Besides, the Raman-like effect of the modulational instability of wave trains, the adverse currents with gradients, and the interactions between wind and wave in the course of swell propagation can also change the swell carrier frequency. Also, the discretization of wave propagation term can cause problems such as the garden sprinkler effect (e.g., Tolman 2002), which might also have some impacts on the swell arrival time.

If the difference in arrival time is due to the errors in energy distribution along frequency in the generation area, or frequency shifting effects during propagation, the delayed/early arrival of a swell event means the swell energy peaks shifted to a higher/lower frequency. However, these effects will not have much impact on the swell peak frequency at the arrival point, as the peak frequency is determined by the spatiotemporal position of the swell source. In this case, there will be no underestimation or overestimation of the peak frequencies at a given time in the model. On the contrary, if the difference is due to the position error of source or the impact of currents such as refraction, the propagation time will be actually shortened or prolonged. Then the delayed/early arrival of a swell event in wave heights will also correspond to a delayed/early arrival in frequency, which will behave as the peak frequency being overestimated/underestimated in the model. In our

dataset, the model on average overestimated the frequency for 1.4%. This seemingly supports the conjecture of the prolonging propagation time. However, the correlation coefficient is calculated between arrival time differences and the average bias of frequency that is found not to be significant. Other parameters including the RMSD of peak frequency, the RMSD of swell direction, and the distance from the storm estimated by the slope of the peak frequency also all give little correlation with the differences in the swell arrival time. Based on the data involved in this study, we cannot underpin physics of swell delay or early arrival, and much more effort is needed to answer this question. All of the above explanations are reasonable so that the arrival time error might be the superposition of many physical processes. More data are needed to split and identify them, particularly the data along swell propagation.

4. Summary

Using the pattern of wave height during a swell event, a methodology of validating the swell arrival time from numerical wave models compared with buoy data was developed. Measurements from the same swell events were organized and identified by tracking the partitioned parameters of the energy spectrum in time. The difference of swell arrival time between the model and buoy is defined using the maximum of cross correlation and the minimum of shifting NRMSD, two consistent estimations. The comparison was made between WW3 hindcast data and NDBC buoys. The result indicated that the wave model has a good prediction of the arrival time of swells, but the swells are on average about 4 h delayed with respect to the model. The present method provides another perspective of evaluating and validating numerical wave model, which could be applied synergistically with other validation methods.

We identified the problem of swell early/late arrival, which is an interesting question itself and deserves much effort. As the swell arrival time is related to both the generation and the propagation of swells, it is a complicated problem and many processes might be responsible for its difference between model and observation. Many possible conjectures having impacts on the swell arrival time are discussed, but we are unable to distinguish between different mechanisms from available data at this stage. Further studies are needed in the future to split the problem and figure out the importance of each factor on the early/late arrival of swells.

REFERENCES

Ardhuin, F., B. Chapron, and F. Collard, 2009: Observation of swell dissipation across oceans. *Geophys. Res. Lett.*, **36**, L06607, doi:10.1029/2008GL037030.

——, and Coauthors, 2010: Semiempirical dissipation source functions for ocean waves. Part I: Definition, calibration, and validation. *J. Phys. Oceanogr.*, **40**, 1917–1941, doi:10.1175/2010JPO4324.1.

——, P. Sutherland, M. Doble, and P. Wadhams, 2016: Ocean waves across the Arctic: Attenuation due to dissipation dominates over scattering for periods longer than 19 s. *Geophys. Res. Lett.*, **43**, 5775–5783, doi:10.1002/2016GL068204.

Babanin, A. V., 2012: Swell attenuation due to wave-induced turbulence. *Proc. 31st Int. Conf. on Ocean, Offshore and Arctic Engineering Division*, Rio de Janeiro, Brazil, American Society of Mechanical Engineers, 439–443, doi:10.1115/OMAE2012-83706.

Barber, N. F., and F. Ursell, 1948: The generation and propagation of ocean waves and swell. I. Wave periods and velocities. *Philos. Trans. Roy. Soc. London*, **A240**, 527–560, doi:10.1098/rsta.1948.0005.

Collard, F., F. Ardhuin, and B. Chapron, 2009: Monitoring and analysis of ocean swell fields from space: New methods for routine observations. *J. Geophys. Res.*, **114**, C07023, doi:10.1029/2008JC005215.

Delpey, M., T. F. Ardhuin, F. Collard, and B. Chapron, 2010: Space-time structure of long ocean swell fields. *J. Geophys. Res.*, **115**, C12037, doi:10.1029/2009JC005885.

Earle, M. D., K. E. Steele, and D. W. C. Wang, 1999: Use of advanced directional wave spectra analysis methods. *Ocean Eng.*, **26**, 1421–1434, doi:10.1016/S0029-8018(99)00010-4.

Gallet, B., and W. R. Young, 2014: Refraction of swell by surface currents. *J. Mar. Res.*, **72**, 105–126, doi:10.1357/002224014813758959.

Hanson, J. L., and O. M. Phillips, 2001: Automated analysis of ocean surface directional wave spectra. *J. Atmos. Oceanic Technol.*, **18**, 277–293, doi:10.1175/1520-0426(2001)018<0277:AAOOSD>2.0.CO;2.

Munk, W. H., G. R. Miller, F. E. Snodgrass, and N. F. Barber, 1963: Directional recording of swell from distant storms. *Philos. Trans. Roy. Soc. London*, **A255**, 505–584, doi:10.1098/rsta.1963.0011.

Portilla, J., F. J. Ocampo-Torres, and J. Monbaliu, 2009: Spectral partitioning and identification of wind sea and swell. *J. Atmos. Oceanic Technol.*, **26**, 107–122, doi:10.1175/2008JTECHO609.1.

Rascle, N., and F. Ardhuin, 2013: A global wave parameter database for geophysical applications. Part 2: Model validation with improved source term parameterization. *Ocean Modell.*, **70**, 174–188, doi:10.1016/j.ocemod.2012.12.001.

Rogers, W. E., J. D. Dykes, and P. A. Wittmann, 2014: US Navy global and regional wave modeling. *Oceanography*, **27**, 56–67, doi:10.5670/oceanog.2014.68.

Snodgrass, F. E., G. W. Groves, K. Hasselmann, G. R. Miller, W. H. Munk, and W. H. Powers, 1966: Propagation of ocean swell

across the Pacific. *Philos. Trans. Roy. Soc. London*, **A249**, 431–497, doi:10.1098/rsta.1966.0022.

Stopa, J. E., F. Ardhuin, A. V. Babanin, and S. Zieger, 2015: Comparison and validation of physical wave parameterizations in spectral wave models. *Ocean Modell.*, **103**, 2–17, doi:10.1016/j.ocemod.2015.09.003.

Tolman, H. L., 2002: Alleviating the garden sprinkler effect in wind wave models. *Ocean Modell.*, **4**, 269–289, doi:10.1016/S1463-5003(02)00004-5.

Wingeart, K. M., T. H. C. Herbers, W. C. O'Reilly, P. A. Wittmann, R. E. Jensen, and H. L. Tolman, 2001: Validation of operational global wave prediction models with spectral buoy data. *Proc. Fourth Int. Symp. Ocean Wave Measurement and Analysis*, San Francisco, CA, ASCE, 590–599, doi:10.1061/40604(273)61.

Zieger, S., A. V. Babanin, W. E. Rogers, and I. R. Young, 2015: Observation-based source terms in the third-generation wave model WAVEWATCH. *Ocean Modell.*, **96**, 2–25, doi:10.1016/j.ocemod.2015.07.014.